LA-UR- $08-7212$

Title:	Scale dependence of sorption coefficients for contaminant transport in saturated fractured rock
Author(s):	Zhenxue Dai, Andrew Wolfsberg, Zhiming Lu, and Hailin Deng Earth and Environmental Sciences Division Los Alamos National Laboratory, NM 87545.
Intended for:	Geophysical Research Letters

Los Alamos
NATIONAL LABORATORY
———— EST.1943 ————

Scale dependence of sorption coefficients for contaminant transport in saturated fractured rock

Zhenxue Dai, Andrew Wolfsberg, Zhiming Lu, and Hailin Deng

Earth and Environmental Sciences Division, Los Alamos National Laboratory
Los Alamos, NM 87545 (email: daiz@lanl.gov)

Abstract: A significant challenge in contaminant transport modeling is to obtain a mechanistic understanding of transport parameter scaling that accurately addresses the combined influence of physical and chemical heterogeneities at different scales. In this paper, we have developed a scaling methodology to upscale matrix sorption coefficients for fractured-rock systems by characterizing both the tortuosity field (physical heterogeneity) and retardation factor field (chemical heterogeneity) in the rock matrix. We compute the effective tortuosity with a conservative tracer (e.g. tritium), and then using a sorbing tracer (e.g. uranium), we derive the equations for upscaling the sorption coefficients in a saturated, fractured rock system. The derived upscaling equations for the sorption coefficients are verified with Monte Carlo simulations, which are based on a generalized dual-porosity model to enable highly efficient and accurate numerical simulations of diffusive concentration fronts moving between the fractures and matrix material. The scientific results from this study will provide a theoretical and practical link between controlled experimental results at scales increasing from the laboratory bench to the field scale at which risk assessment and contaminant remediation are actually conducted.

1. Introduction

Spatial variations of the reactive transport parameters in porous media have been studied at variable scales ranging from column experiments to field tracer tests (e.g. Ginn, 1999; Xu et al., 1999; Yeh, 2000; Davis et al., 2004; Dai and Samper, 2006; Dai et al., 2006; Robinson et al., 2007). Scale dependence of the transport parameters such as retardation factors in porous media has been addressed by Bellin et al. (1993), Rajaram (1997), and Fernàndez-Garcia et al. (2005). Using a Lagrangian approach, Rajaram (1997) defined the effective retardation factors in temporal and spatial domains, and derived the theoretical expressions for these effective factors by assuming the spatial correlations between log conductivity and log retardation factor fields. His results indicate that retardation factors vary with scale, and at large temporal and spatial scales, the effective retardation factor approaches the arithmetic mean of the random retardation factor field. Fernàndez-Garcia et al. (2005) obtained similar conclusions of the scale dependence of the effective retardation factors in the three-dimensional physically and chemically heterogeneous porous media. More studies on the scaling of the retardation factors in porous media have been performed by Robin et al. (1991), Tompson (1993), Burr et al. (1994), Cvetkovic and Dagan (1994), Chao et al. (2000), Andersson et al. (2004), and Samper and Yang (2006).

When dealing with sorption in fractured rock, we obtain a substantially different conceptual model than for porous media. In saturated fractured rock systems where the primary pathway for groundwater flow is through the fractures, the matrix material is saturated with groundwater and is considered immobile in the dual-porosity conceptual model (Tang et al., 1981; Sudicky and Frind, 1982). Although the bulk of the water travels through the fractures, a very large reservoir of water in the matrix can act to store

2

contaminants temporarily via matrix diffusion and sorption processes. If a contaminant sorbs onto the matrix material for a period of time, its transport rate in the fractures is effectively retarded (Robinson, 1994). Studies on the scaling of transport parameters in fractured rock have been conducted by Berkowitz and Scher (1998), Reimus et al. (2003), Cvetkovic et al. (2004), Dai et al. (2007), Liu et al. (2007) and Frampton and Cvetkovic et al. (2007). A mass transfer coefficient was defined by Reimus et al. (2003) to describe the rate at which a particular solute transfers between fractures and the rock matrix material when both diffusion and sorption are involved. The mass transfer coefficient depends on the matrix diffusion coefficient, retardation factor, fracture aperture, and matrix porosity. Therefore, the mass transfer coefficient is a lumped parameter that describes a critical component of reactive contaminant transport in fractured rock systems (advection and dispersion in the fractures being the other components).

The scaling of the retardation factor of a chemical species is related to the variability of the sorption coefficients in the rock mineral facies (e.g. Allen-King et al., 2006; Zavarin et al., 2004). Without an applicable upscaling rule, the parameters controlling sorption under field conditions usually are approximated by the values derived from column experiments. Because the parameters are spatially heterogeneous at various scales, characterization of the physical and chemical heterogeneities that control sorption processes is required. Then, the upscaling equations are derived to upscale the transport parameters from the measurement scale to field or modeling grid scales. In this study, we develop an upscaling methodology for modeling sorption in fractured rock at the field scale. Monte Carlo simulations are performed to demonstrate the accuracy of the derived upscaling algorithms for the effective sorption coefficient.

2. Transport Equations in Fractured Rock

Fracture-matrix transport can be modeled with the one-dimensional advection-dispersion equation with one-dimensional diffusion occurring into the surrounding matrix perpendicular to the flow direction in the fracture (Reimus et al., 2003). The controlling transport equations in fracture and matrix are:

Fracture:

$$R_f \frac{\partial C_f}{\partial t} + v_f \frac{\partial C_f}{\partial x} - D_f \frac{\partial^2 C_f}{\partial x^2} - \frac{\phi D_m}{b\eta} \frac{\partial C_m}{\partial z}\bigg|_{z=b} = 0 \tag{1a}$$

Matrix:

$$R_m \frac{\partial C_m}{\partial t} - D_m \frac{\partial^2 C_m}{\partial z^2} = 0 \tag{1b}$$

where C_f and C_m are the tracer concentrations in the fracture and matrix, respectively; v_f is the fluid velocity in the fracture (in x direction); D_f is the dispersion coefficient in the fracture; D_m is the matrix diffusion coefficient in z direction; R_f and R_m are the retardation factors in the fracture and matrix, respectively; η and ϕ are the porosity in the fracture and matrix, respectively; and b is the fracture half aperture.

Reimus et al. (2003) utilized semi-analytical methods to solve Equations (1), and derived an equation to represent the mass transfer between the fracture and matrix as:

$$C_{MT} = \frac{\tilde{\phi}\sqrt{\tilde{D}_m \tilde{R}_m}}{\tilde{b}\eta} . \tag{2}$$

Equation (2) states that the effective mass transfer coefficient (C_{MT}) at the field scale can be computed based on the effective diffusion coefficient ($\tilde{D}_m$), effective retardation factor ($\tilde{R}_m$, for non-reactive species $\tilde{R}_m = 1$), effective matrix porosity ($\tilde{\phi}$), effective fracture half aperture ($\tilde{b}$) and the fracture porosity. The fracture porosity in most cases can be assumed

4

equal to 1, and the matrix diffusion coefficient can be expressed as $\tilde{D}_m = \tilde{\tau} D_0$, where $\tilde{\tau}$ is the effective matrix tortuosity, and D_0 is the molecular diffusion coefficient in free water. Then, equation (2) is reformed as:

$$C_{MT} = \frac{\tilde{\phi}\sqrt{D_0 \tilde{\tau} \tilde{R}_m}}{\tilde{b}}. \tag{3}$$

3. Effective Retardation Factor

In heterogeneous matrix material, the tortuosity and retardation factor can be expressed as two one-dimensional (along the flow direction), second-order stationary spatial random variables, $Y(x) = \ln R_m$ and $Z(x) = \ln \tau$. The tortuosity random field represents the physical heterogeneity in the matrix, and the retardation factor random field describes the chemical heterogeneity of the matrix. If we take the measurement-scale (usually defined from column experiments) mass transfer coefficient as a spatial random variable, the field-scale mass transfer coefficient can be expressed as the volume average of measurement-scale mass transfer coefficients,

$$\frac{\tilde{\phi}\sqrt{D_0 \tilde{\tau} \tilde{R}_m}}{\tilde{b}} = \frac{1}{L}\int_L \frac{\phi\sqrt{D_0 \tau R_m}}{b}dx. \tag{4}$$

where L is the length of the one-dimensional domain and x is the spatial coordinate. By replacing the measurement-scale porosity (ϕ) and the half aperture (b) with their effective values $\tilde{\phi}$ and $\tilde{b}$ (which are assumed to be estimated separately), we have

$$\tilde{\tau}\tilde{R}_m = \left(\frac{1}{L}\int_L e^{\frac{1}{2}(Y(x)+Z(x))}dx\right)^2. \tag{5}$$

Decomposing $Y(x)$ and $Z(x)$ as the mean M_Y and M_Z, and zero-mean

perturbation $Y'(x)$ and $Z'(x)$, $Y(x) = M_Y + Y'(x)$ and $Z(x) = M_Z + Z'(x)$, we rewrite (5) as a

double integral in the one-dimensional domain,

$$\tilde{\tau}\tilde{R}_m = \frac{R_m^G \tau^G}{L^2} \left(\int_L \int_L e^{\frac{1}{2}(Y'(x)+Y'(y)+Z'(x)+Z'(y))} dx dy \right),$$ (6)

where $R_m^G = e^{M_Y}$ and $\tau^G = e^{M_Z}$ are the geometric means of measurement-scale retardation

factor and tortuosity, and y is also a one-dimensional spatial variable. By using Taylor

expansion and assuming the variance of $Y(x)$ and $Z(x)$ smaller than unity, we have,

$$\langle \tilde{\tau}\tilde{R}_m \rangle = R_m^G \tau^G \left(1 + \frac{\sigma_Y^2 + \sigma_Z^2}{4} + \frac{1}{4L^2} \left(\int_L \int_L (C_Y(x,y) + C_Z(x,y) + \omega_{YZ}(x,y)) dx dy \right) \right),$$ (7)

where, operator $\langle \ \rangle$ represents expectation, σ_Y^2 and σ_Z^2 are variances of log retardation

factor and log tortuosity, $C_Y(x,y) = \langle Y'(x)Y'(y) \rangle$ and $C_Z(x,y) = \langle Z'(x)Z'(y) \rangle$ are their

covariances, respectively, and $\omega_{YZ}(x,y) = \langle Y'(x)Z'(x) + Y'(x)Z'(y) + Y'(y)Z'(y) + Y'(y)Z'(x) \rangle$

is the cross-covariance of retardation factor and tortuosity. We assume that the retardation

factor and tortuosity are not correlated, then $\omega_{YZ}(x,y) = 0$. The covariance functions of the

log retardation factor and log tortuosity can be expressed as:

$$C_Y(h) = \sigma_Y^2 e^{-\frac{h}{\lambda_Y}}, \quad C_Z(h) = \sigma_Z^2 e^{-\frac{h}{\lambda_Z}},$$ (8)

where the lag distance $h = |x - y|$, λ_Y and λ_Z are integral scales of log retardation factor and

log tortuosity. Then, evaluating the integral in equation (7), we have

6

$$\left\langle \tilde{\tau} \tilde{R}_m \right\rangle = R_m^G \tau^G \left(1 + \frac{\sigma_Y^{\ 2} + \sigma_Z^{\ 2}}{4} + \frac{1}{2L^2} \left[\sigma_Y^2 \lambda_Y^2 (\frac{L}{\lambda_Y} - 1 + e^{-\frac{L}{\lambda_Y}}) + \sigma_Z^2 \lambda_Z^2 (\frac{L}{\lambda_Z} - 1 + e^{-\frac{L}{\lambda_Z}}) \right] \right). \qquad (9)$$

Equation (9) represents a combined scaling effect of tortuosity and retardation factor. In order to obtain the effective tortuosity and the effective retardation factor individually, we assume the effective tortuosity is only related to the heterogeneity of the matrix, but not related to the type of solutes (e.g. conservative or reactive tracers). Then, we can use two steps to define the two effective parameters. First, we assume R_m is equal to 1 for a conservative tracer (such as tritium) to define the effective tortuosity, then

$$\left\langle \tilde{\tau} \right\rangle = \tau^G \left(1 + \frac{\sigma_Z^{\ 2}}{4} + \frac{\sigma_Z^2 \lambda_Z^2}{2L^2} (\frac{L}{\lambda_Z} - 1 + e^{-\frac{L}{\lambda_Z}}) \right). \qquad (10)$$

Equation (10) is similar to the effective matrix diffusion equations in Dai et al. (2007) because these two parameters are related by $\tilde{D}_m = \tilde{\tau} D_0$. Second, after defining the effective tortuosity, we can compute the effective R_m of a sorbing tracer (such as uranium) as:

$$\left\langle \tilde{R}_m \right\rangle = R_m^G \left(1 + \frac{\sigma_Y^{\ 2} \tau^G}{4 \left\langle \tilde{\tau} \right\rangle} \left(1 + \frac{2\lambda_Y^2}{L^2} (\frac{L}{\lambda_Y} - 1 + e^{-\frac{L}{\lambda_Y}}) \right) \right). \qquad (11)$$

Equation (11) indicates that the effective retardation factor increases with the variance of $Y(x)$ in the matrix. If the matrix is homogeneous, the variance is 0, and the effective R_m is equal to the geometric mean, which indicates that the physical and chemical heterogeneities of matrix properties are the source of the scale dependence of retardation factor.

4. Effective Sorption Coefficient

The effective sorption coefficient can be computed from the effective retardation factor from the equation:

$$\tilde{K}_d = (\tilde{R}_m - 1) \frac{\tilde{\phi}}{\rho}, \qquad (12)$$

7

where, $\tilde{K}_d$ is the effective sorption coefficient, and ρ is the dry density of the matrix

material. By replacing the effective retardation factor in (12) with (11), we obtain an

expression for the effective sorption coefficient,

$$\tilde{K}_d = \frac{\tilde{\phi}R_m^G}{\rho}\left(\left(1+\frac{\sigma_Y^2 \tau^G}{4\langle\tilde{\tau}\rangle}\left(1+\frac{2\lambda_Y^2}{L^2}(\frac{L}{\lambda_Y}-1+e^{-\frac{L}{\lambda_Y}})\right)\right)-\frac{1}{R_m^G}\right).$$

(13)

A synthetic field-scale heterogeneous matrix system is built to investigate the scale

dependence of K_d, and the corresponding statistical parameters are listed in Table 1. The

diffusion coefficient and retardation factor represent uranium (a sorbing tracer) and are

abstracted from Wolfsberg et al. (2002). Using (13) and the data listed in Table 1, we plot the

effective K_d vs. the integral scale in curve A of Figure 1, which shows that the effective K_d

increases with the increasing integral scales. When the integral scale is 300 m, the

corresponding effective K_d is 4.7 cm^3/g, which is 19% larger than its geometric mean (3.95

cm^3/g). Curve B of Figure 1 shows that the effective K_d decreases with the ratio of domain

size and integral scale. This result indicates that if the integral scale is a constant, when the

domain size increases, the effective K_d decreases approaching the geometric mean as the

likelihood of sampling all possible K_ds increases.

Furthermore, if $\lambda_Y / L \to 0$, which means the field is not correlated or $Y(x)$ is totally

randomly distributed, (13) is approximated as:

$$\tilde{K}_d = \frac{\tilde{\phi}R_m^G}{\rho}\left(1+\frac{\sigma_Y^2 \tau^G}{4\langle\tilde{\tau}\rangle}-\frac{1}{R_m^G}\right).$$

(14)

On the other hand, if λ_Y / L is sufficiently large, (13) is approximated as:

8

$$\tilde{K}_d = \frac{\tilde{\phi} R_m^G}{\rho} \left(1 + \frac{\sigma_Y^2 \tau^G}{2\langle \tilde{\tau} \rangle} - \frac{1}{R_m^G} \right).$$ (15)

These two equations represent the minimum and the maximum of the effective K_d, which are illustrated in the Figure 1.

5. Monte Carlo Simulations

Monte Carlo simulations are conducted to assess the accuracy of the upscaling equations of the sorption coefficients in fractured rocks with the generalized double porosity model (GDPM, Zyvoloski et al., 2008). The GDPM numerical model has a length of 1000 m, a fracture spacing of 2 m, and a half aperture of 0.01 m. The model has 1001 fracture nodes (uniform resolution in direction of flow $\Delta x = 1$ m) and 10010 matrix nodes (each fracture node connects to 10 matrix nodes perpendicular to the flow direction with variable spatial spaces from 0.01 to 0.4 m, see Figure 2). The inflow water has a constant injection rate of 0.012 kg/s. In the inflow water, the solute concentration of uranium is normalized to 1.

There are two spatial random variables, tortuosity $Z(x)$ and retardation factor $Y(x)$ to represent the physical and chemical heterogeneities of the matrix. The heterogeneous fields of $Z(x)$ and $Y(x)$ were generated with a Gaussian random field generator (Lu and Zhang, 2004). We generated 5000 realizations with the statistical data listed in Table 1. The quality of the generated fields was checked by comparing the covariance calculated from the generated realizations with the analytical, exponential covariance model. The comparison shows that the realizations match the specified mean, variance, and integral scale. Then, the generated $Z(x)$ and $Y(x)$ are converted to D_m and K_d for GDPM models.

9

For each Monte Carlo simulation, we use the numerical simulator of GDPM (Zyvoloski et al., 2008) to solve Equation (1) and to compute the concentration breakthrough at the outflow fracture node. The evolutions of concentration mean and variance with the number of simulations are also computed until the solution of the Monte Carlo simulations converges (Figure 3). Figure 4 shows that the concentration breakthrough simulated with the effective K_d calculated from equation (13) matches well to the mean concentration after 5000 Monte Carlo simulations, while with the geometric mean of K_d the concentration is overestimated. This result indicates that the derived effective sorption coefficient is an accurate estimate for the field-scale modeling.

6. Summary and Conclusion

The physical and chemical heterogeneities of matrix properties are a source of the scale dependence of sorption coefficients. The major factors affecting sorption coefficient heterogeneity include matrix porosity, tortuosity, mineral facies and rock units. In this paper, we take the mass transfer coefficient as a lumped spatial random variable to incorporate the variation of all these factors and upscale the sorption coefficient from the laboratory or measurement scale to the field scale.

The effective sorption coefficient is dependent on the geometric mean, variance, integral scale, and domain size. Its value increases with the integral scale and is greater than the geometric mean. The Monte Carlo simulations with 5000 realizations of heterogeneous fields demonstrate that the derived effective sorption coefficient is an accurate estimation of K_d for field-scale transport modeling in saturated fractured rocks. The effective sorption coefficient is derived under the condition that the variance is smaller than unity. Further work is needed to identify the maximum variance that is applicable for the first-order perturbation

method. The next extension of this effort will be to incorporate the more complex physical and chemical heterogeneity such as multimodal mineral facies to test how the multimodal heterogeneity affects the scaling of the sorption coefficients.

References

Allen-King, R. M., D. P. Divine, M. J. L. Robin, J. R. Alldredge, and D. R. Gaylord (2006), Spatial distributions of perchloroethylene reactive transport parameters in the Borden Aquifer, *Water Resour. Res.*, *42*, W01413, doi:10.1029/2005WR003977.

Andersson, P., J. Byegard, E. L. Tullborg, T. Doe, J. Hermanson, and A. Winberge (2004), In situ tracer tests to determine retention properties of a block scale fracture network in granitic rock at the Aspo Hard Rock Laboratory, Sweden, *J. Contam. Hydrol.*, *70*(3–4), 271–297.

Bellin, A., A. Rinaldo, W. Bosma, S. van der Zee, and Y. Rubin (1993), Linear Equilibrium Adsorbing Solute Transport in Physically and Chemically Heterogeneous Porous Formations 1. Analytical Solutions, Water Resour. Res., 29(12), 4019-4030.

Berkowitz, B., and H. Scher (1998), Theory of anomalous chemical transport in random fracture networks, *Phys. Rev. E*, 57(5), 5858–5869.

Burr, D. T., E. A. Sudicky, and R. L. Naff (1994), Nonreactive and reactive solute transport in three-dimensional heterogeneous porous media: Mean displacement, plume spreading, and uncertainty, *Water Resour. Res.*, 30(3), 791–815.

Chao, C.-H., H. Rajaram, and T. H. Illangasekare (2000), Intermediate-scale experiments and numerical simulations of transport under radial flow in a two-dimensional heterogeneous porous medium, *Water Resour. Res.*, 36(10), 2869–2884.

Cvetkovic, V., and G. Dagan (1994), Transport of kinetically sorbing solute by steady random velocity in heterogeneous porous formations, *J. Fluid Mech.*, 265, 189–215.

Cvetkovic, V., S. Painter, N. Outters, and J. O. Selroos (2004), Stochastic simulation of radionuclide migration in discretely fractured rock near the Äspö Hard Rock Laboratory, *Water Resour. Res.*, 40, W02404, doi:10.1029/2003WR002655.

Dai, Z. and J. Samper (2006). Inverse modeling of water flow and multicomponent reactive transport in coastal aquifer systems, *J. of Hydrology*, 327, 447-461.

Dai, Z., J. Samper, and R. Ritzi (2006). Identifying geochemical processes by inverse modeling of multicomponent reactive transport in Aquia aquifer, *Geosphere,* v. 2, no. 4, p.210-219, doi: 10.1130/GES00021.1, June.

Dai, Z., A. Wolfsberg, Z. Lu, and P. Reimus (2007), Upscaling matrix diffusion coefficients for heterogeneous fractured rocks, *Geophys. Res. Lett.*, 34, L07408, doi:10.1029/2007GL029332.

Davis, J.A., S.B. Yabusaki, C.I. Steefel, J.M. Zachara, G.P. Curtis, G.D. Redden, L.J. Criscenti, and B.D. Honey (2004), Assessing conceptual models for subsurface reactive transport of inorganic contaminants, *Transactions of American Geophysical Union* (EOS), v. 85, No. 44, November 2.

Fernàndez-Garcia, D., T. H. Illangasekare, and H. Rajaram (2005), Differences in the scale dependence of dispersivity and retardation factors estimated from forced-gradient and uniform flow tracer tests in three-dimensional physically and chemically heterogeneous porous media, *Water Resour. Res.*, *41*, W03012, doi:10.1029/2004WR003125.

Frampton, A., and V. Cvetkovic (2007), Upscaling particle transport in discrete fracture networks: 2. Reactive tracers, *Water Resour. Res.*, 43, W10429, doi:10.1029/2006WR005336.

Ginn, T.R. (1999), On the distribution of multicomponent mixtures over generalized exposure time in subsurface flow and reactive transport: foundations, and formulations for groundwater age, chemical heterogeneity, and biodegradation, *Water Resour. Res.* 35 (1999), pp. 1395–1407.

Liu, H.H., Y.Q. Zhang, Q. Zhou, F.J. Molz (2007), An interpretation of potential scale dependence of the effective matrix diffusion coefficient, *J. Contam. Hydrol.*, *90*(1–2), 41–57.

Lu, Z. , and D. Zhang (2004), A comparative study on quantifying uncertainty of flow in heterogeneous media using Monte Carlo simulations, the conventional and the KL-based moment-equation approaches, *SIAM J. on Scientific Computing*, 26(2), 558-577.

Rajaram, H. (1997), Time and scale dependent effective retardation factors in heterogeneous aquifers, *Adv. Water Resour.*, 20(4), 217–230.

Reimus P., G. Pohll, T. Mihevc, J. Chapman, M. Haga, B. Lyles, S. Kosinski, R. Niswonger, P. Sanders (2003), Testing and parameterizing a conceptual model for solute transport in a fractured granite using multiple tracers in a forced‐gradient test, *Water Resour. Res.*, 39 (12), 1356, doi:10.1029/2002WR001597.

Robin, M. J. L., E. A. Sudicky, R. W. Gillham, and R. G. Kachanoski (1991), Spatial variability of strontium distribution coefficients and their correlation with hydraulic conductivity in the Canadian forces base Borden aquifer, *Water Resour. Res.*, 27(10), 2619–2632.

Robinson, B. A. (1994), A strategy for validating a conceptual model for radionuclide migration in the saturated zone beneath Yucca Mountain, *Radioactive Waste Management and Environmental Restoration*, Vol. 19, pp. 73-96.

Robinson B. A., A. V. Wolfsberg, H. S. Viswanathan, P. W. Reimus (2007), A colloid-facilitated transport model with variable colloid transport properties, *Geophys. Res. Lett.*, 34, L09401, doi:10.1029/2007GL029625.

Samper, J. and C. Yang (2006), Stochastic analysis of transport and multicomponent competitive monovalent cation exchange in aquifers, *Geosphere*; April 2006; v. 2; no. 2; p. 102–112; doi: 10.1130/GES00030.1.

Tompson, A. F. B. (1993), Numerical simulation of chemical migration in physically and chemically heterogeneous porous media, *Water Resour. Res.*, 29(11), 3709–3726.

Wolfsberg, A., L. Glascoe, G. Lu, A. Olson, P. Lichtner, M. McGraw, T. Cherry, and G. Roemer (2002), TYBO/BENHAM Model Analysis of Groundwater Flow and Radionuclide Migration from Underground Nuclear Tests in Southwestern Pahute Mesa, NTS, LA-13977, 424 p, Los Alamos, NM: Los Alamos National Laboratory.

Xu, T., J. Samper, C. Ayora, M. Manzano and E. Custodio (1999), Modeling of non-isothermal multicomponent reactive transport in field scale porous media flow systems, *J. of Hydrol.*, Vol. 214, 144-164.

Yeh, G.T. (2000), Computational subsurface hydrology, reactions, transport and fate: The Netherlands, Kluwer Academic Publishers, 318 p.

Zavarin, M., S. F. Carle, and R. M. Maxwell (2004), Upscaling Radionuclide Retardation—Linking the Surface Complexation and Ion Exchange Mechanistic Approach to a Linear Kd Approach, UCRL-TR-204713, Lawrence Livermore National Laboratory, Livermore, California.

Zyvoloski, G.A., B.A. Robinson, and H.S. Viswanathan, (2008), Generalized double porosity: A numerical method for representing spatially variable sub-grid scale processes, *Adv. Water Resour.*, 31, Issue 3, p.535–544.

List of Table

Table 1. The statistical parameters for a synthetic heterogeneous matrix system

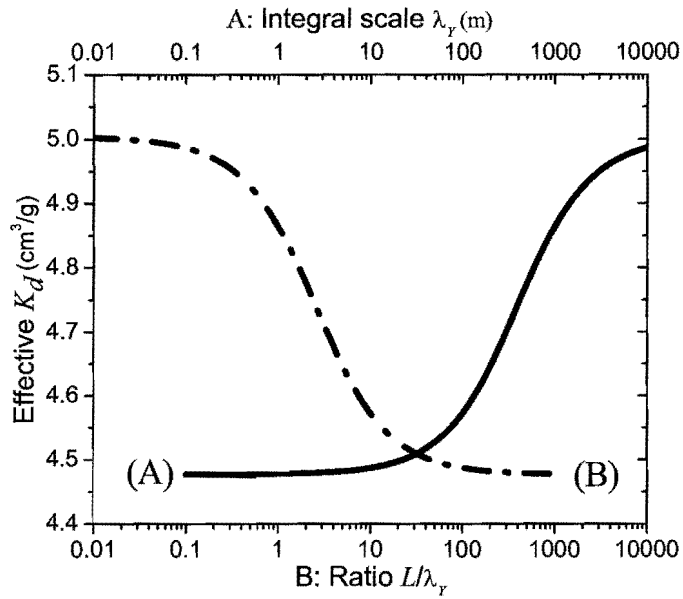| Parameters	Mean of $Y(x)$ or $Z(x)$	Variance of $Y(x)$ or $Z(x)$	Geometric mean	Integral scale (m)	Effective values
τ	-3.615	0.4	0.0269	200	0.0309
D_m (m^2/s)	N/A	N/A	1.78×10^{-11}	N/A	2.05×10^{-11}
R_m	3.919	0.6	50.375	300	59.77
K_d (cm^3/g)	N/A	N/A	3.95	N/A	4.702
$D_0 = 6.64\times10^{-11}$ m^2/s, $\rho = 2.5$ g/cm^3, ϕ =0.2 and $L = 1000$ m.					

List of Figure Captions

Figure 1. Effective K_d increases with the integral scale (curve A) and it decreases with the ratio of domain size and integral scale (curve B).
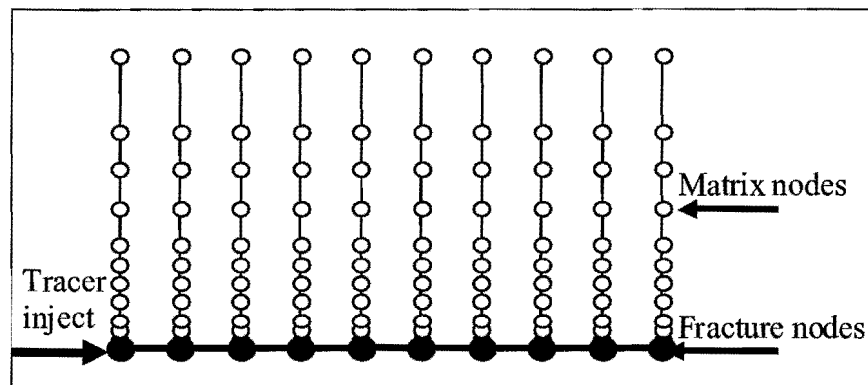
Figure 2. A conceptual illustration for the numerical grids of a generalized double porosity model. The tortuosity and sorption coefficient in the matrix are heterogeneous.

Figure 3. The computed mean concentration (left) and variance (right) with the number of the Monte Carlo simulations at 1500 days in the outflow fracture node.

Figure 4. Comparison of the concentration breakthrough curves computed from the effective K_d, geometric mean K_d and the Monte Carlo simulations, respectively.

Figure 1. Effective K_d increases with the integral scale (curve A) and it decreases with the ratio of domain size and integral scale (curve B).

Figure 2. A conceptual illustration for the numerical grids of a generalized double porosity model. The tortuosity and sorption coefficient in the matrix are heterogeneous.
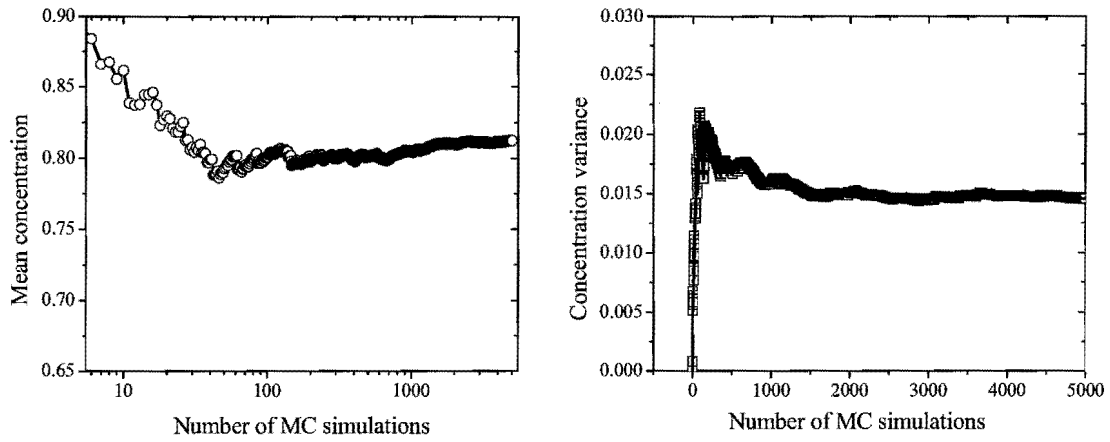
Figure 3. The computed mean concentration (left) and variance (right) with the number of the Monte Carlo simulations at 1500 days in the outflow fracture node.
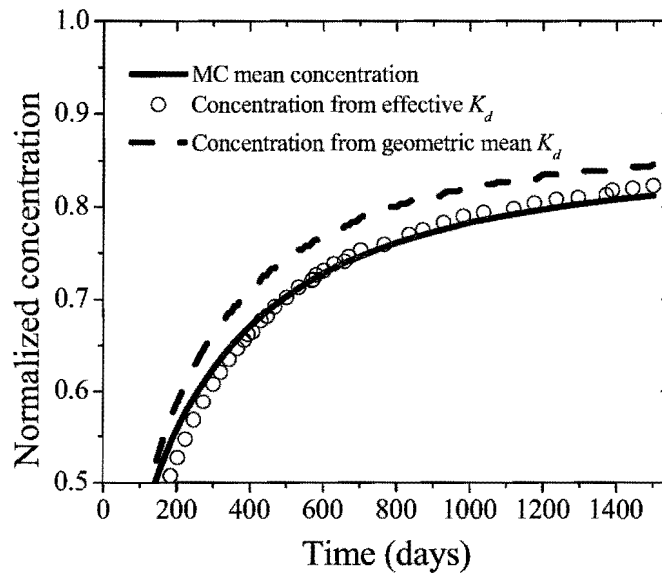

Figure 4. Comparison of the concentration breakthrough curves computed from the effective K_d, geometric mean K_d and the Monte Carlo simulations, respectively.